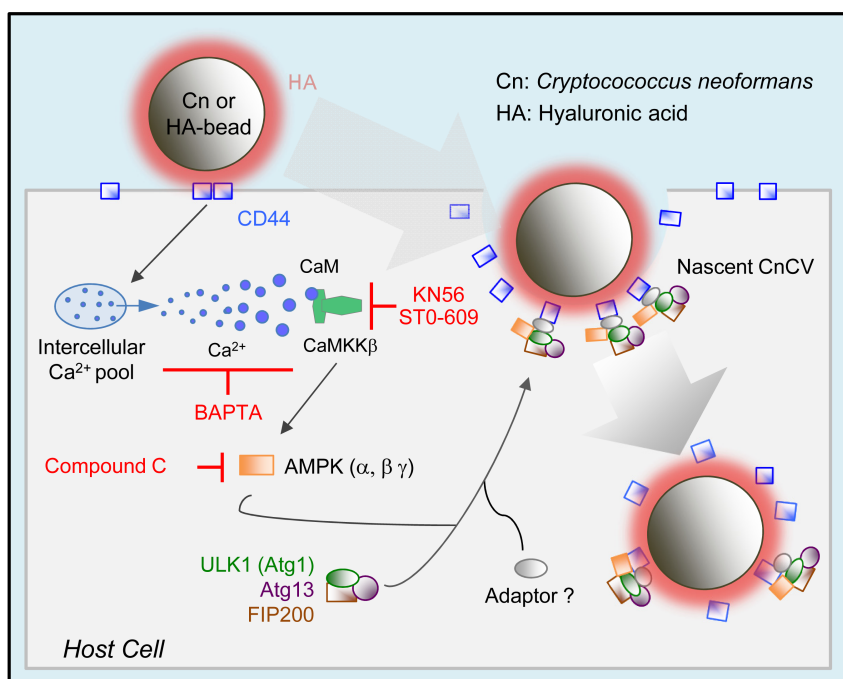


Interactions Between Fungal Hyaluronic Acid and Host CD44 Promote Internalization by Recruiting Host Autophagy Proteins to Forming Phagosomes

Graphical Abstract



Authors

Sheng Li Ding, Aseem Pandey, Xuehuan Feng, ... , Qing-Ming Qin, Thomas A. Ficht, Paul de Figueiredo

Correspondence

qm Qin@jlu.edu.cn (Q.M.Q.),
tficht@tamu.edu (T.A.F.),
pjdefigueiredo@tamu.edu (P.d.F.)

In Brief

Ding et al. reveal that interactions between fungal hyaluronic acid (HA) and host CD44 activate a Ca²⁺-CaMKKβ-AMPK-ULK1 signaling pathway that recruits autophagy initiation complex components to forming phagosomes to drive fungal internalization.

Highlights

- Fungal HA interactions with host cells drive a novel non-canonical, ligand-induced, autophagy pathway in phagocytic cells
- *Cryptococcus neoformans* recruits host CD44, together with AIC components and regulatory proteins, to forming phagocytic cups to initiate host cell internalization
- Fungal HA interactions with CD44 on host cell surfaces elevate intracellular Ca²⁺ concentrations, leading to activation of CaMKKβ
- A Ca²⁺-CaMKKβ-AMPK-ULK1 signaling axis is involved in HA and CD44 induced autophagy protein recruitment during Cn internalization

1 **Interactions between fungal hyaluronic acid and host CD44 promote**
2 **internalization by recruiting host autophagy proteins to forming phagosomes**

3
4 Sheng Li Ding^{1,2,6}, Aseem Pandey^{2,3,6}, Xuehuan Feng^{2,6}, Jing Yang², Luciana Fachini da Costa^{2,4},
5 Roula Mouneimne³, Allison Rice-Ficht⁴, Samantha L. Bell⁵, Robert O. Watson⁵, Kristin Patrick⁵,
6 Qing-Ming Qin^{1,2*}, Thomas A. Ficht^{3*}, Paul de Figueiredo^{2,3,7*}

7
8 ¹ College of Plant Sciences & Key Laboratory of Zoonosis Research, Ministry of Education, Jilin
9 University, Changchun 130062, Jilin, China; Department of Plant Pathology, College of Plant
10 Protection, Henan Agricultural University, Zhengzhou 450002, Henan, China

11 ² Department of Microbial Pathogenesis and Immunology, Texas A&M Health Science Center,
12 Norman Borlaug Center, Texas A&M University, College Station, Texas 77843, USA

13 ³ Department of Veterinary Pathobiology, Texas A&M University, College Station, Texas 77843,
14 USA

15 ⁴ Department of Molecular and Cellular Medicine, College of Medicine, Texas A&M Health
16 Science Center, College Station, Texas 77843, USA

17 ⁵ Department of Microbial Pathogenesis and Immunology, Texas A&M Health Science Center,
18 Bryan, Texas 77807, USA

19 ⁶ These authors contributed equally

20 ⁷ Lead contact

21 * Correspondence: qm Qin@jlu.edu.cn (Q.M.Q.), tficht@tamu.edu (T.A.F.), pjdefigueiredo@tamu.edu (P.d.F.)

22
23
24

1 **Summary**

2
3 Phagocytosis and autophagy play critical roles in immune defense. *Cryptococcus neoformans* (Cn),
4 a fungal pathogen that causes fatal infection, subverts the host autophagy initiation complex (AIC)
5 and its upstream regulatory proteins, to promote its phagocytosis and intracellular parasitism of
6 host cells. The mechanisms by which the pathogen engages host AIC proteins remain obscure.
7 Here, we show that the recruitment of host AIC proteins to forming phagosomes is dependent
8 upon the activity of CD44, a host cell surface receptor that engages fungal hyaluronic acid (HA).
9 This interaction elevates intracellular Ca^{2+} concentrations and activates CaMKK β and its
10 downstream target AMPK α , which results in activation of ULK1 and the recruitment of AIC
11 components. Moreover, we demonstrate that HA-coated beads efficiently recruit AIC components
12 to phagosomes. Taken together, these findings show that fungal HA plays a critical role in
13 directing the internalization and productive intracellular membrane trafficking of a fungal
14 pathogen of global importance.

15

16

1 **Introduction**

2
3 Autophagy is an orderly “self-eating” process in cells that coordinates the degradation of cellular
4 components. Various types of autophagy have been described, including macrophagy, microphagy,
5 mitophagy, chaperone-mediated autophagy and xenophagy (Galluzzi et al., 2017; Khandia et al.,
6 2019; Kirkin and Rogov, 2019). Some pathogens subvert autophagic machinery to promote their
7 intracellular survival and replication (Case et al., 2016; de Figueiredo and Dickman, 2016; de
8 Figueiredo et al., 2015; Dickman et al., 2017; Pandey et al., 2018). Several signaling pathways
9 control the onset, duration and outcome of autophagy induction in mammalian cells (Abada and
10 Elazar, 2014; Rubinsztein et al., 2012). Pathways that include components of the autophagy
11 initiation complex (AIC), including AMPK, ULK1, ATG13, FIP200 and ATG9, play important
12 roles in these processes (Ganley et al., 2009; Hosokawa et al., 2009; Jung et al., 2009). For
13 example, AMPK or ULK1 signaling can regulate ATG9 recruitment to nascent phagosome or
14 autophagosome membranes (Mack et al., 2012). This recruitment process is believed to contribute
15 to the elongation of the autophagosomal membrane (Mack et al., 2012).

16
17 *Cryptococcus neoformans* (Cn) is a pathogen of global consequence that causes fatal fungal
18 meningoencephalitis worldwide (Kozubowski and Heitman, 2012; Olszewski et al., 2010; Sabiiti
19 and May, 2012). Cn is particularly pernicious in immunocompromised individuals, where lethal
20 infection constitutes a significant risk (Warkentien and Crum-Cianflone, 2010). Cn can survive,
21 replicate and persist in both intracellular and extracellular environments within mammalian hosts
22 (Garcia-Rodas and Zaragoza, 2012). However, the molecular mechanisms that control intracellular
23 parasitism remain poorly understood (Evans et al., 2018; Zaragoza, 2019). Towards addressing
24 this issue, we reported a functional analysis of host factors that regulate the infection, intracellular
25 replication, and non-lytic release of Cn from host cells (Qin et al., 2011). We extended these
26 findings by performing a phosphoproteomic analysis of the host response to Cn infection (Pandey
27 et al., 2017). This analysis demonstrated that host AIC proteins, and upstream regulatory
28 molecules, contribute to the internalization and intracellular replication of the pathogen in
29 macrophages (Pandey et al., 2017). This work also raised questions about the cellular and
30 molecular mechanisms by which these proteins contribute to this phenotype.

31

1 The internalization of Cn into host cells is regulated, in part, by interactions between fungal
2 components and host associated CD44, a major receptor for hyaluronic acid (HA) in mammalian
3 cells (Jong et al., 2012; Jong et al., 2008). Moreover, CD44 has been shown to control
4 phagocytosis of the pathogen (Jong et al., 2012; Jong et al., 2008). Interestingly, mice deficient for
5 CD44 display reduced susceptibility to infection (Jong et al., 2012). The deficiency in
6 phagocytosis accounts for this phenotype, leaving open the question of the mechanism by which
7 CD44 controls fungal internalization. Here, we show that Cn phagocytosis by macrophages occurs
8 by a novel mechanism whereby AIC proteins, including ULK1, ATG9 and ATG13, as well as the
9 key upstream signaling component AMPK α , are recruited to forming phagosomes to promote the
10 phagocytosis of the pathogen in a CD44-dependent fashion. Interaction of fungal HA and host
11 CD44 activates a Ca²⁺-CaMKK β (calcium/calmodulin-dependent protein kinase kinase β subunit)-
12 AMPK-ULK1 signaling axis that supports Cn internalization into host cells. Taken together, our
13 findings uncover unexpected roles for HA-CD44 interactions in conferring susceptibility to fungal
14 infection and open up new avenues for therapeutic intervention for a fungal pathogen of global
15 importance.

16

17 **Results**

18

19 **Cn recruits host AIC components to forming Cn-containing phagosomes**

20 To test the hypothesis that Cn infection of macrophages promotes the formation of a physical
21 complex that contains AIC components, we used Forster Resonance Energy Transfer (FRET)
22 imaging microscopy, which detects close molecular associations (< 10 nm) (Irving et al., 2014), to
23 measure such interactions. The quenching of fluorescence in the donor fluorophore of a FRET pair
24 accompanies the establishment of a close physical association between the pairs (Irving et al.,
25 2014). We measured photon transfer between antibody labeled ATG13 and ULK1 or AMPK α and
26 FIP200 in infected and uninfected RAW264.7 macrophages. We observed significant increases in
27 the amount of FRET between these proteins in infected cells (**Figure S1A-D**). However,
28 comparable FRET interactions were not observed in controls that were stained with a single label,
29 or in uninfected samples (**Figure S1A-D**), thereby indicating the establishment of a close
30 association between these proteins during infection.

31

1 **Recruitment of AIC components to forming phagosomes containing Cn is galectin 8** 2 **independent**

3 Previous studies have shown that galectin 8, a β -galactoside-binding lectin, monitors endosomal
4 and lysosomal integrity by binding to host glycans on damaged pathogen-containing vacuoles.
5 This binding drives the ubiquitin-dependent recruitment of autophagy adaptor proteins (e.g.,
6 NDP52) and microtubule associated light chain kinase 3 (LC3), which in turn, promotes the
7 recruitment of autophagosome biogenesis proteins to damaged pathogen-containing vacuoles
8 (Thurston et al., 2012). Galectin 8 mediated autophagosomal targeting is relevant to the observed
9 recruitment of AIC components to phagocytic cups because Cn containing vacuoles (CnCVs) are
10 permeabilized after phagocytosis by macrophages (Johnston and May, 2010). Moreover, nascent
11 CnCVs in infected macrophages recruit host LC3 (Fig. S1E) (Nicola et al., 2012; Qin et al., 2011),
12 thereby implicating trafficking pathways that recruit LC3 to phagosomal membranes in controlling
13 the intracellular lifestyle of Cn. With these ideas in mind, we tested the hypothesis that AIC
14 recruitment to nascent CnCVs is associated with galectin 8 recruitment to these subcellular
15 structures. We infected RAW264.7 macrophages that express a GFP-tagged variant of galectin 8
16 (GFP-Gal8) with Cn, and then used immunofluorescence microscopy (IFM) to determine whether
17 GFP-Gal8 colocalized with AMPK α on nascent phagosomes containing Cn cells. We found that
18 GFP-Gal8 did not display quantitative colocalization with either AMPK α or nascent phagosomes
19 (Figure S1F). Consistent with these observations was the finding that UBEI-41, a potent and cell-
20 permeable inhibitor of ubiquitin E1 activity (Yang et al., 2007), when added to macrophages at
21 non-toxic doses (30 μ M), did not diminish AIC recruitment to CnCVs (Figure S1G). Importantly,
22 the inhibitor was washed out of the host cell culture media before Cn infection, thereby ensuring
23 that the drug only targeted host cell components in these experiments. In addition, we found that
24 nascent phagosomes decorated with the AIC component ULK1 colocalized with the endosomal
25 marker EEA1 (Figure S1H). We also found that calreticulin, a Ca²⁺ binding ER (endoplasmic
26 reticulum) protein, was recruited to phagocytic cups and nascent CnCVs (Figure S1I), and that
27 LC3 displayed minimal colocalization with AIC components on nascent CnCVs (Figure S1J, left).
28 CnCVs in B6J2 macrophages expressing dominant negative variants of the AIC regulatory
29 component AMPK α recruited less LC3 (Figure S1J, right) and AIC components (Figure S1K),
30 thereby suggesting that AIC recruitment to nascent Cn-containing phagosomes and LC3
31 recruitment to phagosome membranes could be morphologically and genetically dissected. Taken

1 together, these findings indicated that recruitment of AIC to the nascent phagosomes and the
2 induction of autophagy were galectin 8-independent events.

3
4 **A non-proteinaceous and/or non-capsular component controls AIC recruitment to nascent**
5 **CnCVs**

6 The observation that AIC and AIC regulatory components were recruited to forming phagosomes
7 during Cn infection of macrophages encouraged us to determine the mechanism of recruitment.
8 We infected host cells with live or dead Cn and found that fungal viability was not required for
9 AIC recruitment because nascent CnCVs containing the heat-killed (HK) organism also efficiently
10 recruited these proteins (**Figure 1A**). These observations were consistent with the hypothesis that
11 non-proteinaceous, Cn-associated molecules activate the host AIC pathway.

12
13 Cn is encased in a carbohydrate-enriched capsule that is essential for intracellular parasitism and
14 virulence (O'Meara and Alspaugh, 2012). To test the hypothesis that capsular components direct
15 the recruitment of AIC and AIC regulatory proteins to forming phagosomes, we infected host cells
16 with an acapsular mutant of Cn (Cap59), which displays defects in extracellular trafficking of
17 glucuronoxylomannan (GXM) (Garcia-Rivera et al., 2004), and analyzed AIC recruitment to
18 phagosomes containing cap59 strains. We found that forming and formed phagosomes that
19 contained the acapsular strain also efficiently recruited AIC proteins (**Figure 1B-D, Figure S2A-**
20 **C**). AIC components showed close associations with internalized Cn cells as detected by indirect
21 immunofluorescence with anti-capsular monoclonal antibody 18B7 (Garcia-Rivera et al., 2004)
22 (**Figure S2D**). Moreover, infection of host cells with live wild-type (WT) Cn resulted in the
23 activation by phosphorylation of host cell ULK1 (Ser555), a key component of the AIC, and
24 activation of the AIC regulatory protein AMPK α (Thr172) (Pandey et al., 2017). Similarly, the
25 acapsular mutant and HK Cn also activated host AMPK α (Thr172) and/or ULK1 (**Figure 1E-H,**
26 **Figure S2E**). However, when *S. cerevisiae* was incubated with host cells, similar AIC recruitment
27 was not observed (**Figure S2F**), suggesting that phagocytosis of yeast cells by macrophages
28 involves the participation of a distinct mechanism. Taken together, these findings suggested that
29 Cn-specific, non-proteinaceous, non-capsular components activated the host AMPK-ULK1
30 signaling axis and promoted AIC recruitment to forming phagosomes.

31

1 **CD44-deficient host cells fail to recruit AIC proteins to forming phagosomes**

2 CD44 regulates fungal internalization (Jong et al., 2012; Jong et al., 2008). This observation raised
3 the intriguing possibility that CD44 interactions with other host cell components may also control
4 the recruitment of AIC components to nascent CnCVs. To test this hypothesis, we first used
5 fluorescence microscopy to determine whether CD44 colocalized with Cn cells or was recruited to
6 forming or formed nascent CnCVs. We also tested whether CD44 deficient macrophages recruited
7 AIC components to the nascent pathogen-containing phagosomes. We found that forming or
8 formed phagosomes containing both capsular or acapsular strains displayed strong colocalization
9 with CD44 (**Figure 2A**), and that CD44 was enriched at sites of contact between the pathogen and
10 the host cell surface during a time course of infection (**Figure S2G**). Next, we tested whether
11 CD44 colocalized with AIC regulatory AMPK and AIC components on nascent CnCVs. We
12 found that AIC components, including ATG9 and ULK1, colocalized with CD44 on nascent
13 CnCVs (**Figure 2B-C**). Compared to CD44^{+/+} bone-marrow derived macrophage (BMDM)
14 controls, AMPK α showed reduced colocalization in CD44^{-/-} BMDMs (**Figure 2D**). As a result, Cn
15 internalization in CD44-deficient cells was reduced (**Figure 2E-F**), indicating that host cell CD44
16 is required for Cn internalization, and that activation of the AMPK-ULK1 signaling axis and AIC
17 recruitment is CD44-dependent.

18

19 ***cpsI* deletion mutants fail to recruit AIC components to nascent CnCVs**

20 HA, a component of the Cn cell wall, is known to interact with CD44, an HA receptor on host
21 cells, and to promote the internalization of the pathogen into human and murine brain
22 microvascular endothelial cells (BMECs) (Jong et al., 2012; Jong et al., 2008). This observation
23 raised the intriguing possibility that HA-CD44 interactions may promote the recruitment of AIC
24 components to nascent CnCVs. To test this hypothesis, we first examined the internalization of Cn
25 strains that harbor mutations in *cpsI*, a gene that encodes hyaluronic synthase (Jong et al., 2007).
26 Consistent with previous findings where Cn displayed reduced association with CD44-depleted
27 murine BMECs compared to controls (Jong et al., 2012), we found that deletion of *cpsI* displayed
28 reduced internalization of Cn into host macrophages (**Figure 3A-C, Figure S3A**). Next, we used
29 fluorescence microscopy to determine whether *cpsI*-deficient Cn strains recruited AIC
30 components to nascent pathogen-containing phagosomes. We found the mutant strain displayed
31 reduced recruitment compared to WT controls (**Figure 3D**). However, nascent CnCVs that

1 contained strain C558 (*cps1Δ::CPS1*), in which the *cps1* mutation was complemented with a WT
2 copy of the gene (Jong et al., 2008), displayed higher levels of AIC recruitment than their CPS1-
3 deficient counterparts (Figure 3D). These data suggested that HA, the product of *cps1* activity,
4 contributed to directing the recruitment of AIC components to nascent CnCVs, and implicated a
5 role for CD44, the dominant HA receptor on macrophages, in regulating this process.

6 7 **Pathogen-derived HA drives interactions between CD44 and AIC components**

8 To test whether HA was sufficient to induce CD44-mediated recruitment of AIC components to
9 nascent CnCVs, we determined whether HA-coated beads induced similar recruitment to forming
10 phagosomes. For these experiments, we covalently coupled HA to polystyrene beads and then
11 incubated the HA-coupled beads with RAW264.7 macrophages for various lengths of time. We
12 also used antibodies directed against AIC components in immunofluorescence microscopy
13 experiments to visualize the recruitment of AIC components to forming phagosomes that
14 contained beads. We found robust recruitment of AMPK α and AIC component ULK1 to forming
15 phagosomes containing HA-coated beads (Figure 3E-H). We also incubated HA-coated beads
16 with GFP-Gal8 expressing macrophages and found that recruitment of AMPK α or galectin 8 to
17 the sites of bead internalization was not detected (Figure S3B, upper). However, co-localization
18 of CD44 and AMPK α was observed to be colocalized with the HA-coated beads (Figure S3B,
19 lower). Our observations therefore suggested that HA interactions with CD44 were necessary and
20 sufficient to induce the formation of an AIC protein complex on forming phagosomes.

21 22 **Interaction of fungal HA with host CD44 activates AMPK and AIC pathways**

23 The observation that interactions between HA and host CD44 recruited AIC components to
24 forming phagosomes raised questions about the mechanism of AIC recruitment by these
25 components. HA induces Ca²⁺ elevation in cells and may increase the activity of Ca²⁺-associated
26 signaling pathways (Singleton and Bourguignon, 2002). For example, an increase of cytoplasmic
27 Ca²⁺ levels can induce autophagy through CaMKK β and AMPK pathways (Feng et al., 2020;
28 Green et al., 2011). To test whether HA and CD44 interactions elevate intracellular Ca²⁺ ([Ca²⁺]_i)
29 levels and induce autophagy by Ca²⁺-mediated activation of CaMKK β and AMPK pathways, we
30 incubated host cells with Cn cells, HA, naked beads, or HA-coated beads, and then visualized
31 [Ca²⁺]_i levels and activation of CaMKK β -AMPK pathways in the treated cells. We observed that

1 compared to the controls, *cps1*⁺-Cn induced Ca²⁺-fluxes and increased [Ca²⁺]_i concentrations in a
2 pulsed manner (**Figure 4A-C; Videos 1-2**). Similar results were observed in cells incubated with
3 HA or HA-coated beads (**Figure S3C**), which is consistent with results from a previous report
4 ([Singleton and Bourguignon, 2002](#)). Corresponding to the increase of [Ca²⁺]_i levels, activation of
5 CaMKKβ and AMPKα was observed in H99 cells, ([Pandey et al., 2017](#)), or HA or HA-coated
6 beads (**Figure 4D-E**). Importantly, phosphorylated AMPKα and ATG9 were co-
7 immunoprecipitated from host cells incubated with HA-coated, but not naked, beads (**Figure 4F**).
8
9 To test whether activation of AMPK resulted from the increase of [Ca²⁺]_i, we treated host cells
10 with or without supplementation of assorted inhibitors, including BAPTA-AM (a [Ca²⁺]_i-chelator),
11 KN62 (a specific CaMK inhibitor), and STO-609 (a specific CaMKKα/β inhibitor), during
12 infection with Cn. We found that host cells treated with these compounds displayed reduced
13 activation of AMPK (**Figure 4G**); the activation of the downstream target ULK1 was also almost
14 completely blocked (**Figure 4H**). During Cn infection, ULK1 is activated in a p-AMPK-
15 dependent fashion (**Figure 4G-I**). Consequently, Cn internalization was reduced in cells in which
16 [Ca²⁺]_i was chelated, the activities of CaMK or CaMKKα/β were inhibited or depleted (**Figure 4J**;
17 **Figure S4A-D**), or AMPK or AIC components were depleted (**Figure S4E-F**). These findings
18 suggest that interaction of HA with CD44 recruits AIC to forming phagosomes by release of Ca²⁺
19 and activation of the CaMKKβ-AMPK-ULK1 signaling axis.

20 21 **Discussion**

22
23 The intracellular lifestyle of Cn is pivotal for pathogen colonization, dissemination and disease
24 progression ([Garcia-Rodas and Zaragoza, 2012](#); [Johnston and May, 2013](#); [Seider et al., 2010](#)), as
25 well as establishment of latent infection ([Saha et al., 2007](#)). Although the complete set of host
26 factors that regulate intracellular parasitism remain obscure, published reports demonstrate that
27 both “zipper” (receptor-mediated) and “trigger” (membrane ruffle dependent) mechanisms
28 contribute to the internalization of Cn ([Guerra et al., 2014](#)). Moreover, interactions between the
29 opsonized or unopsonized pathogen and host cell surface receptors are important to these
30 processes ([Shoham et al., 2001](#); [Taborda and Casadevall, 2002](#)). The findings reported here
31 provide a new understanding of phagocytic mechanisms by demonstrating that fungal HA- and

1 host CD44-dependent recruitment of AIC network components to nascent CnCVs play a central
2 role in regulating the internalization of the fungus. Cn cells, opsonized or unopsonized and live or
3 dead, as well as HA-coated beads, efficiently recruited host CD44, components of AIC and its
4 regulatory protein AMPK to forming or formed phagosomes. As such, this report provides the first
5 example of ligand- and receptor-induced recruitment of AIC proteins, including ULK1, FIP200,
6 ATG13, and ATG9, to nascent phagosomes in macrophages.

7
8 Host cell galectin 8 is involved in defending against bacterial infection by recruiting the
9 autophagic adaptor NDP52 to damaged *Salmonella*-containing vacuoles and in activating
10 antibacterial autophagy (Thurston et al., 2012). Different from the defensive autophagy induced by
11 galectin 8, significant recruitment of the danger receptor galectin 8 to forming or formed
12 phagosomes during Cn internalization and/or intracellular replication was not observed,
13 suggesting that a different strategy is employed to recruit elements of the autophagy machinery
14 through interactions between fungal HA and host cell CD44. Besides AMPK and AIC components,
15 the endosomal and lysosomal markers EEA1, M6PR, and Cathepsin D, as well as the ER marker
16 calreticulin, were recruited to nascent phagosomes (Qin et al., 2011). Interestingly, co-localization
17 of the endocytic marker EEA1 and the AIC component ULK1 was also observed, suggesting that
18 the endosomal and lysosomal pathways, ER-derived membrane and selective autophagy
19 machinery are involved in the internalization of Cn into host cells. How these factors coordinate
20 this process and the involvement of other ubiquitin-binding autophagic adaptors related to the AIC
21 remain to be characterized.

22
23 AMPK can be activated by cellular stresses that elevate AMP levels by means of allosteric binding
24 of AMP to sites in the γ subunit AMPK, and by phosphorylation of Thr172 in AMPK α by the
25 tumor suppressor LKB1, CaMKK β , or the transforming growth factor- β -activated kinase (TAK1)
26 (Hardie et al., 2012; Kola et al., 2006; Zadra et al., 2015). Activation of AMPK can induce
27 autophagy via direct phosphorylation of ULK1 (Egan et al., 2011; Kim et al., 2011; Zhao and
28 Klionsky, 2011). Previous observations showed that HA interactions with CD44 induces Ca²⁺
29 elevation in cells (Singleton and Bourguignon, 2002), and that increases in cytoplasmic Ca²⁺
30 concentrations induce autophagy through activation of CaMKK β and AMPK pathways (Feng et
31 al., 2020; Green et al., 2011). Similarly, our findings demonstrate that infection by Cn recruits

1 host cell CD44 to CnCVs, induces intracellular Ca^{2+} -flux in the infected host cells, activates
2 CaMKK β and AMPK, and recruits AIC components to forming or nascent CnCVs. Cn infection
3 also activates LKB1, and depletion of LKB1 reduced Cn internalization into host cells ([Pandey et
4 al., 2017](#)). However, how the interaction of HA and CD44 activates AMPK through the upstream
5 regulatory proteins LKB1 and TAK1 remains to be further characterized.

6
7 Our data support a stepwise model in which several sequential molecular events control the
8 internalization of Cn in macrophages. First, interactions between fungal HA and CD44 on the
9 surface of host cells stimulates the release of Ca^{2+} and elevates intercellular Ca^{2+} levels, which
10 results in the activation of CaMKK β and AMPK. Second, phosphorylation of ULK1 occurs in an
11 AMPK-dependent fashion. Third, AMPK-dependent activation of ULK1 recruits AIC components,
12 including the ULK1-ATG13-FIP200 complex, ATG9, and LC3, to forming phagocytic cups
13 containing the fungus. Fourth, the coordinated activities of AIC components drive the
14 internalization of the pathogen into host cells. Finally, AIC component interactions with CnCVs
15 gradually diminish as the pathogen establishes a replicative niche in host cells (**Figure for
16 graphical Abstract**).

17
18 Finally, it is notable that several proteins in AMPK α and AIC regulatory networks are targets of
19 commonly prescribed drugs (e.g., AMPK, a target for metformin) or under development as targets
20 for pharmaceutical intervention (e.g., ULK1) ([Egan et al., 2015](#)). Several fungi, including *Candida*
21 spp. and *Histoplasma capsulatum*, are capable of intracellular parasitism ([Garcia-Rodas et al.,
22 2011](#); [Howard, 1965](#); [Woods, 2003](#)). Therefore, our findings may open up new therapeutic
23 possibilities for preventing cryptococcosis and other infections caused by intracellular pathogens.

24 25 **Acknowledgement**

26 We gratefully thank Arturo Casadevall (Department of Microbiology and Immunology, Albert
27 Einstein College of Medicine, Yeshiva University) for anti-cryptococcal antibodies, and Steve
28 Fullwood and Kalli Landua (Nikon Instruments) for expert assistance with the microscopy
29 analysis. This work is supported by the Texas AM Clinical Science Translational Research
30 Institute Pilot Grant CSTR2016-1, DARPA (HR001118A0025-FoF-FP-006), NIH
31 (R21AI139738-01A1, 1 R01AI141607-01A1, 1R21GM132705-01), the National Science

1 Foundation (DBI 1532188, NSF0854684) and the Bill Melinda Gates Foundation, the Defense
2 Advanced Research Projects Agency (Agreement HR001118A0025-FoF-FP-006) to PdF; NIH
3 grant awards NIH 1R01 AI48496-01A1 and NIH 1U54AI057156-0100 to TAF; the National
4 Natural Science Foundation of China (# 81371773) to QMQ. Any opinions, findings, and
5 conclusions or recommendations expressed in this material are those of the author(s) and do not
6 necessarily reflect the views of the funding agencies.

7 8 **Author Contributions**

9 P.D., Q.M.Q., T.A.F. designed the experiments. S.L.D., A.P., X.H.F., Q.M.Q, J.Y., L.F.d.C., R.M.
10 S.L.B. performed experiments. P.D., T.A.F., A.R., R.M., R.O.W., K.P. provided reagents/analysis
11 tools. P.D., Q.M.Q., S.L.D., X.H.F., A.P., T.A.F. analyzed data. P.D., Q.M.Q. supervised the work
12 and wrote the manuscript.

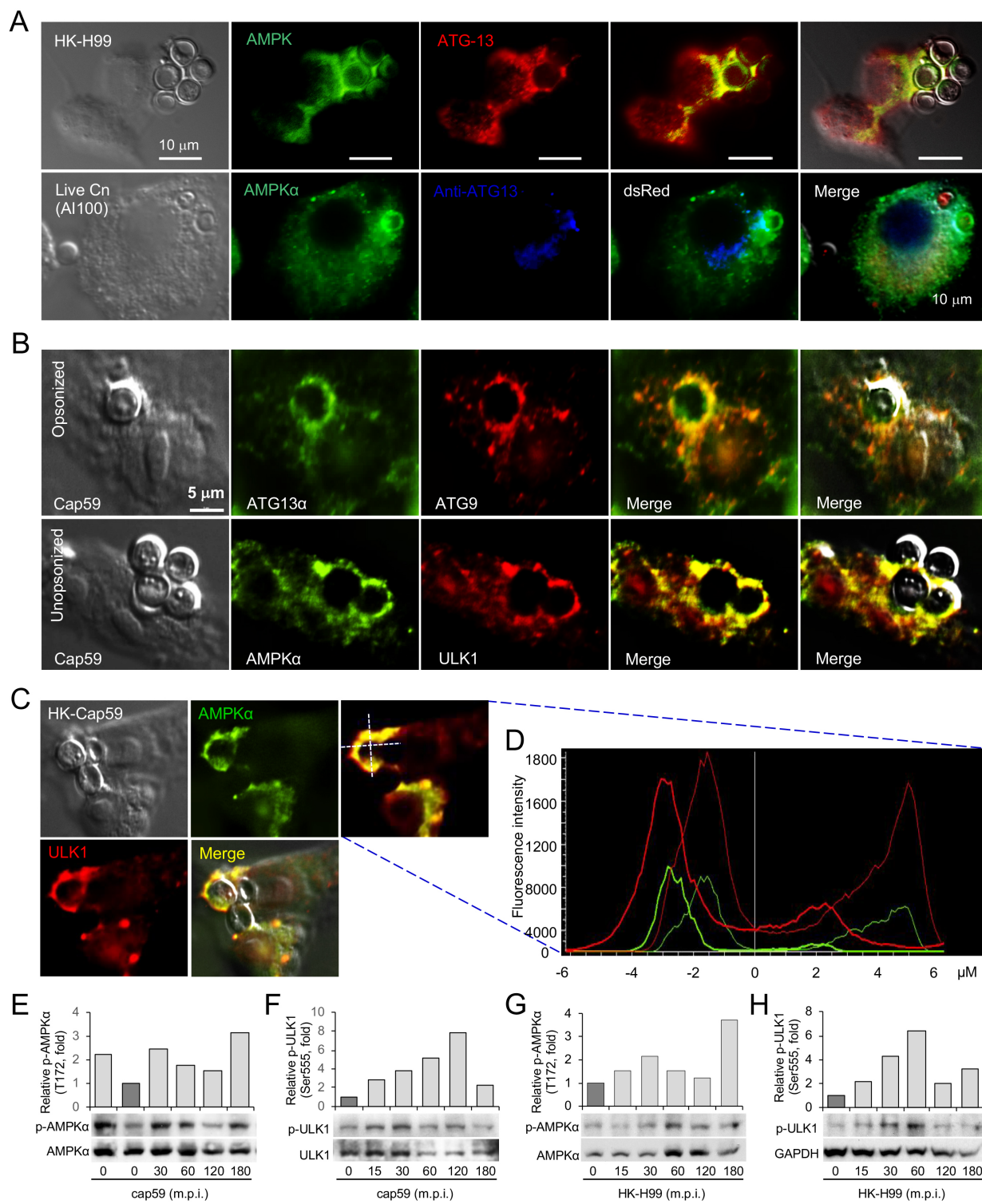
13 14 **References**

- 15
16 Abada, A., and Elazar, Z. (2014). Getting ready for building: signaling and autophagosome biogenesis. *EMBO*
17 *Rep.*
18 Campeau, E., Ruhl, V.E., Rodier, F., Smith, C.L., Rahmberg, B.L., Fuss, J.O., Campisi, J., Yaswen, P., Cooper,
19 P.K., and Kaufman, P.D. (2009). A versatile viral system for expression and depletion of proteins in
20 mammalian cells. *PLoS one* 4.
21 Case, E.D.R., Smith, J.A., Ficht, T.A., Samuel, J.E., and de Figueiredo, P. (2016). Space: a final frontier for
22 vacuolar pathogens. *Traffic* 17, 461-474.
23 de Figueiredo, P., and Dickman, M. (2016). Plant Disease: Autophagy under attack. *eLife* 5, e14447.
24 de Figueiredo, P., Ficht, T.A., Rice-Ficht, A., Rossetti, C.A., and Adams, L.G. (2015). Pathogenesis and
25 immunobiology of brucellosis: review of Brucella–Host Interactions. *The American journal of pathology* 185,
26 1505-1517.
27 Dickman, M., Williams, B., Li, Y., de Figueiredo, P., and Wolpert, T. (2017). Reassessing apoptosis in plants.
28 *Nature plants* 3, 773-779.
29 Egan, D.F., Chun, M.G., Vamos, M., Zou, H., Rong, J., Miller, C.J., Lou, H.J., Raveendra-Panickar, D., Yang,
30 C.C., Sheffler, D.J., *et al.* (2015). Small Molecule Inhibition of the Autophagy Kinase ULK1 and
31 Identification of ULK1 Substrates. *Mol Cell* 59, 285-297.
32 Egan, D.F., Shackelford, D.B., Mihaylova, M.M., Gelino, S., Kohnz, R.A., Mair, W., Vasquez, D.S., Joshi, A.,
33 Gwinn, D.M., and Taylor, R. (2011). Phosphorylation of ULK1 (hATG1) by AMP-activated protein kinase
34 connects energy sensing to mitophagy. *Science* 331, 456-461.
35 Evans, R.J., Sundaramurthy, V., and Frickel, E.-M. (2018). The interplay of host autophagy and eukaryotic
36 pathogens. *Frontiers in Cell and Developmental Biology* 6, 118.
37 Feng, N., Wang, B., Cai, P., Zheng, W., Zou, H., Gu, J., Yuan, Y., Liu, X., Liu, Z., and Bian, J. (2020). ZEA-
38 induced autophagy in TM4 cells was mediated by the release of Ca²⁺ activates CaMKK β -AMPK signaling
39 pathway in the endoplasmic reticulum. *Toxicology Letters*.
40 Galluzzi, L., Baehrecke, E.H., Ballabio, A., Boya, P., Bravo-San Pedro, J.M., Cecconi, F., Choi, A.M., Chu,
41 C.T., Codogno, P., and Colombo, M.I. (2017). Molecular definitions of autophagy and related processes. *The*
42 *EMBO journal* 36, 1811-1836.

- 1 Ganley, I.G., Lam, D.H., Wang, J., Ding, X., Chen, S., and Jiang, X. (2009). ULK1· ATG13· FIP200 complex
2 mediates mTOR signaling and is essential for autophagy. *Journal of Biological Chemistry* 284, 12297-12305.
- 3 Garcia-Rivera, J., Chang, Y.C., Kwon-Chung, K.J., and Casadevall, A. (2004). Cryptococcus neoformans
4 CAP59 (or Cap59p) is involved in the extracellular trafficking of capsular glucuronoxylomannan. *Eukaryot*
5 *Cell* 3, 385-392.
- 6 Garcia-Rodas, R., Gonzalez-Camacho, F., Rodriguez-Tudela, J.L., Cuenca-Estrella, M., and Zaragoza, O. (2011).
7 The interaction between Candida krusei and murine macrophages results in multiple outcomes, including
8 intracellular survival and escape from killing. *Infect Immun* 79, 2136-2144.
- 9 Garcia-Rodas, R., and Zaragoza, O. (2012). Catch me if you can: phagocytosis and killing avoidance by
10 Cryptococcus neoformans. *FEMS Immunol Med Microbiol* 64, 147-161.
- 11 Green, M.F., Anderson, K.A., and Means, A.R. (2011). Characterization of the CaMKK β -AMPK signaling
12 complex. *Cellular signalling* 23, 2005-2012.
- 13 Guerra, C.R., Seabra, S.H., de Souza, W., and Rozental, S. (2014). Cryptococcus neoformans is internalized by
14 receptor-mediated or 'triggered' phagocytosis, dependent on actin recruitment. *PLoS One* 9, e89250.
- 15 Hardie, D.G., Ross, F.A., and Hawley, S.A. (2012). AMPK: a nutrient and energy sensor that maintains energy
16 homeostasis. *Nature reviews Molecular cell biology* 13, 251-262.
- 17 Hosokawa, N., Hara, T., Kaizuka, T., Kishi, C., Takamura, A., Miura, Y., Iemura, S.-i., Natsume, T., Takehana,
18 K., and Yamada, N. (2009). Nutrient-dependent mTORC1 association with the ULK1-Atg13-FIP200
19 complex required for autophagy. *Molecular biology of the cell* 20, 1981-1991.
- 20 Howard, D.H. (1965). Intracellular Growth of Histoplasma Capsulatum. *J Bacteriol* 89, 518-523.
- 21 Irving, A.T., Mimuro, H., Kufer, T.A., Lo, C., Wheeler, R., Turner, L.J., Thomas, B.J., Malosse, C., Gantier,
22 M.P., Casillas, L.N., *et al.* (2014). The immune receptor NOD1 and kinase RIP2 interact with bacterial
23 peptidoglycan on early endosomes to promote autophagy and inflammatory signaling. *Cell host & microbe*
24 *15*, 623-635.
- 25 Johnston, S.A., and May, R.C. (2010). The human fungal pathogen Cryptococcus neoformans escapes
26 macrophages by a phagosome emptying mechanism that is inhibited by Arp2/3 complex-mediated actin
27 polymerisation. *PLoS Pathog* 6, e1001041.
- 28 Johnston, S.A., and May, R.C. (2013). Cryptococcus interactions with macrophages: evasion and manipulation
29 of the phagosome by a fungal pathogen. *Cell Microbiol* 15, 403-411.
- 30 Jong, A., Wu, C.H., Chen, H.M., Luo, F., Kwon-Chung, K.J., Chang, Y.C., Lamunyon, C.W., Plaas, A., and
31 Huang, S.H. (2007). Identification and characterization of CPS1 as a hyaluronic acid synthase contributing
32 to the pathogenesis of Cryptococcus neoformans infection. *Eukaryot Cell* 6, 1486-1496.
- 33 Jong, A., Wu, C.H., Gonzales-Gomez, I., Kwon-Chung, K.J., Chang, Y.C., Tseng, H.K., Cho, W.L., and Huang,
34 S.H. (2012). Hyaluronic acid receptor CD44 deficiency is associated with decreased Cryptococcus
35 neoformans brain infection. *J Biol Chem* 287, 15298-15306.
- 36 Jong, A., Wu, C.H., Shackelford, G.M., Kwon-Chung, K.J., Chang, Y.C., Chen, H.M., Ouyang, Y., and Huang,
37 S.H. (2008). Involvement of human CD44 during Cryptococcus neoformans infection of brain microvascular
38 endothelial cells. *Cellular microbiology* 10, 1313-1326.
- 39 Jung, C.H., Jun, C.B., Ro, S.-H., Kim, Y.-M., Otto, N.M., Cao, J., Kundu, M., and Kim, D.-H. (2009). ULK-
40 Atg13-FIP200 complexes mediate mTOR signaling to the autophagy machinery. *Molecular biology of the*
41 *cell* 20, 1992-2003.
- 42 Khandia, R., Dadar, M., Munjal, A., Dhama, K., Karthik, K., Tiwari, R., Yattoo, M., Iqbal, H., Singh, K.P., and
43 Joshi, S.K. (2019). A comprehensive review of autophagy and its various roles in infectious, non-infectious,
44 and lifestyle diseases: current knowledge and prospects for disease prevention, novel drug design, and
45 therapy. *Cells* 8, 674.
- 46 Kim, J., Kundu, M., Viollet, B., and Guan, K.-L. (2011). AMPK and mTOR regulate autophagy through direct
47 phosphorylation of Ulk1. *Nature cell biology* 13, 132-141.
- 48 Kirkin, V., and Rogov, V.V. (2019). A Diversity of Selective Autophagy Receptors Determines the Specificity
49 of the Autophagy Pathway. *Molecular cell*.
- 50 Kola, B., Boscaro, M., Rutter, G.A., Grossman, A.B., and Korbonits, M. (2006). Expanding role of AMPK in
51 endocrinology. *Trends in Endocrinology & Metabolism* 17, 205-215.
- 52 Kozubowski, L., and Heitman, J. (2012). Profiling a killer, the development of Cryptococcus neoformans.
53 *FEMS Microbiol Rev* 36, 78-94.

- 1 Mack, H.I., Zheng, B., Asara, J.M., and Thomas, S.M. (2012). AMPK-dependent phosphorylation of ULK1
2 regulates ATG9 localization. *Autophagy* 8, 1197-1214.
- 3 Nicola, A.M., Albuquerque, P., Martinez, L.R., Dal-Rosso, R.A., Saylor, C., De Jesus, M., Nosanchuk, J.D., and
4 Casadevall, A. (2012). Macrophage autophagy in immunity to *Cryptococcus neoformans* and *Candida*
5 *albicans*. *Infect Immun* 80, 3065-3076.
- 6 O'Meara, T.R., and Alspaugh, J.A. (2012). The *Cryptococcus neoformans* capsule: a sword and a shield. *Clin*
7 *Microbiol Rev* 25, 387-408.
- 8 Olszewski, M.A., Zhang, Y., and Huffnagle, G.B. (2010). Mechanisms of cryptococcal virulence and persistence.
9 *Future Microbiol* 5, 1269-1288.
- 10 Pandey, A., Ding, S.L., Qin, Q.M., Gupta, R., Gomez, G., Lin, F., Feng, X., Fachini da Costa, L., Chaki, S.P.,
11 Katepalli, M., *et al.* (2017). Global Reprogramming of Host Kinase Signaling in Response to Fungal
12 Infection. *Cell host & microbe* 21, 637-649 e636.
- 13 Pandey, A., Lin, F., Cabello, A.L., da Costa, L.F., Feng, X., Feng, H.-Q., Zhang, M.-Z., Iwawaki, T., Rice-Ficht,
14 A., and Ficht, T.A. (2018). Activation of host IRE1 α -dependent signaling axis contributes the intracellular
15 parasitism of *Brucella melitensis*. *Frontiers in Cellular and Infection Microbiology* 8, 103.
- 16 Qin, Q.M., Luo, J., Lin, X., Pei, J., Li, L., Ficht, T.A., and de Figueiredo, P. (2011). Functional analysis of host
17 factors that mediate the intracellular lifestyle of *Cryptococcus neoformans*. *PLoS Pathog* 7, e1002078.
- 18 Rubinsztein, D.C., Shpilka, T., and Elazar, Z. (2012). Mechanisms of autophagosome biogenesis. *Curr Biol* 22,
19 R29-34.
- 20 Sabiiti, W., and May, R.C. (2012). Mechanisms of infection by the human fungal pathogen *Cryptococcus*
21 *neoformans*. *Future Microbiol* 7, 1297-1313.
- 22 Sag, D., Carling, D., Stout, R.D., and Suttles, J. (2008). Adenosine 5'-monophosphate-activated protein kinase
23 promotes macrophage polarization to an anti-inflammatory functional phenotype. *Journal of immunology*
24 181, 8633-8641.
- 25 Saha, D.C., Goldman, D.L., Shao, X., Casadevall, A., Husain, S., Limaye, A.P., Lyon, M., Somani, J., Pursell,
26 K., Pruett, T.L., *et al.* (2007). Serologic evidence for reactivation of cryptococcosis in solid-organ transplant
27 recipients. *Clin Vaccine Immunol* 14, 1550-1554.
- 28 Seider, K., Heyken, A., Luttich, A., Miramon, P., and Hube, B. (2010). Interaction of pathogenic yeasts with
29 phagocytes: survival, persistence and escape. *Curr Opin Microbiol* 13, 392-400.
- 30 Shoham, S., Huang, C., Chen, J.M., Golenbock, D.T., and Levitz, S.M. (2001). Toll-like receptor 4 mediates
31 intracellular signaling without TNF- α release in response to *Cryptococcus neoformans* polysaccharide
32 capsule. *J Immunol* 166, 4620-4626.
- 33 Singleton, P.A., and Bourguignon, L.Y. (2002). CD44v10 interaction with Rho-kinase (ROK) activates inositol
34 1, 4, 5-triphosphate (IP3) receptor-mediated Ca²⁺ signaling during hyaluronan (HA)-induced endothelial cell
35 migration. *Cell motility and the cytoskeleton* 53, 293-316.
- 36 Tabora, C.P., and Casadevall, A. (2002). CR3 (CD11b/CD18) and CR4 (CD11c/CD18) are involved in
37 complement-independent antibody-mediated phagocytosis of *Cryptococcus neoformans*. *Immunity* 16, 791-
38 802.
- 39 Thurston, T.L., Wandel, M.P., von Muhlinen, N., Foeglein, A., and Randow, F. (2012). Galectin 8 targets
40 damaged vesicles for autophagy to defend cells against bacterial invasion. *Nature* 482, 414-418.
- 41 Warkentien, T., and Crum-Cianflone, N.F. (2010). An update on *Cryptococcus* among HIV-infected patients. *Int*
42 *J STD AIDS* 21, 679-684.
- 43 Woods, J.P. (2003). Knocking on the right door and making a comfortable home: *Histoplasma capsulatum*
44 intracellular pathogenesis. *Curr Opin Microbiol* 6, 327-331.
- 45 Yang, Y., Kitagaki, J., Dai, R.M., Tsai, Y.C., Lorick, K.L., Ludwig, R.L., Pierre, S.A., Jensen, J.P., Davydov,
46 I.V., Oberoi, P., *et al.* (2007). Inhibitors of ubiquitin-activating enzyme (E1), a new class of potential cancer
47 therapeutics. *Cancer Res* 67, 9472-9481.
- 48 Zadra, G., Batista, J.L., and Loda, M. (2015). Dissecting the dual role of AMPK in cancer: from experimental to
49 human studies. *Molecular cancer research* 13, 1059-1072.
- 50 Zaragoza, O. (2019). Basic principles of the virulence of *Cryptococcus*. *Virulence* 10, 490-501.
- 51 Zhao, M., and Klionsky, D.J. (2011). AMPK-dependent phosphorylation of ULK1 induces autophagy. *Cell*
52 *metabolism* 13, 119-120.
- 53

1 Figures and Figure Legends



2

1 **Figure 1. Non-proteineous components on Cn direct the recruitment of host AIC**
2 **components to nascent phagosomes.**

3 (A, B) Colocalization of AMPK α and AIC components surrounding nascent CnCVs in host cells
4 infected with live or heat-killed (HK) H99 (A) and opsonized or unopsonized acapsular cap59
5 strains (B) of Cn.

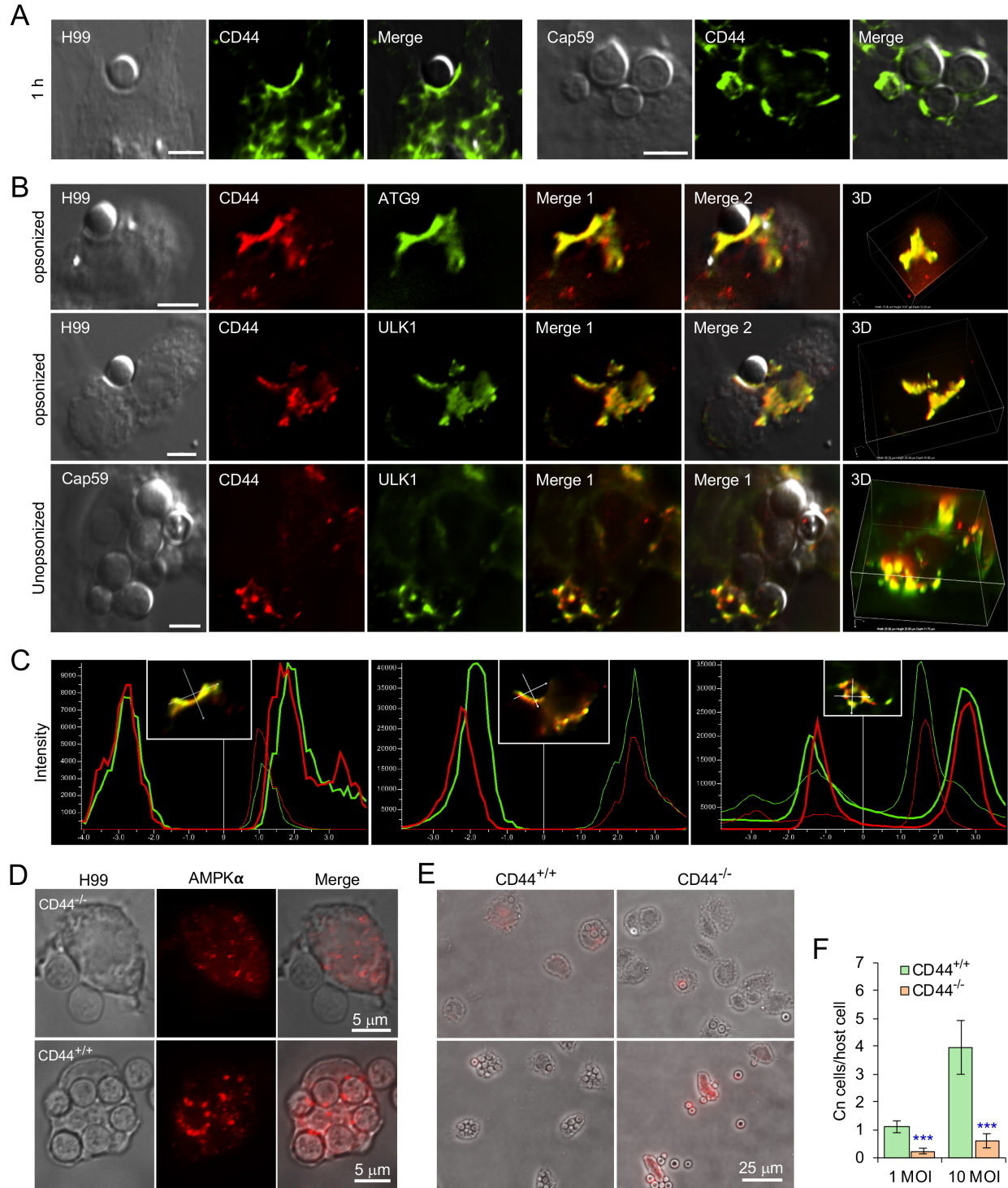
6 (C, D) Recruitment of AMPK α and ULK1 to nascent CnCVs in host cells incubated with HK-
7 cap59 at 3 h.p.i. (C) and the fluorescence intensity profile of AMPK α (green) and ULK1 (red)
8 along the two crossed white lines (D).

9 (E, F) Activation of host cell AMPK α (E) and ULK1 (F) by acapsular Cn strain cap59.

10 (G, H) Activation of host cell AMPK α (G) and ULK1 (H) by HK Cn strain H99 (HK-H99).

11

12



1
2

1 **Figure 2. Host-associated CD44 is required for Cn host cell internalization.**

2 (A) Recruitment of host CD44 to nascent CnCVs that contained the wild-type (WT) strain H99
3 (leaf panel) or acapsular mutant strain cap59 (right panel) of Cn. At 1 hr post-infection (h.p.i.),
4 host cells were fixed, permeabilized and processed for immunofluorescence microscopy using
5 antibodies directed against the indicated host proteins. The antibody-stained samples were then
6 subjected to confocal microscopy image analysis.

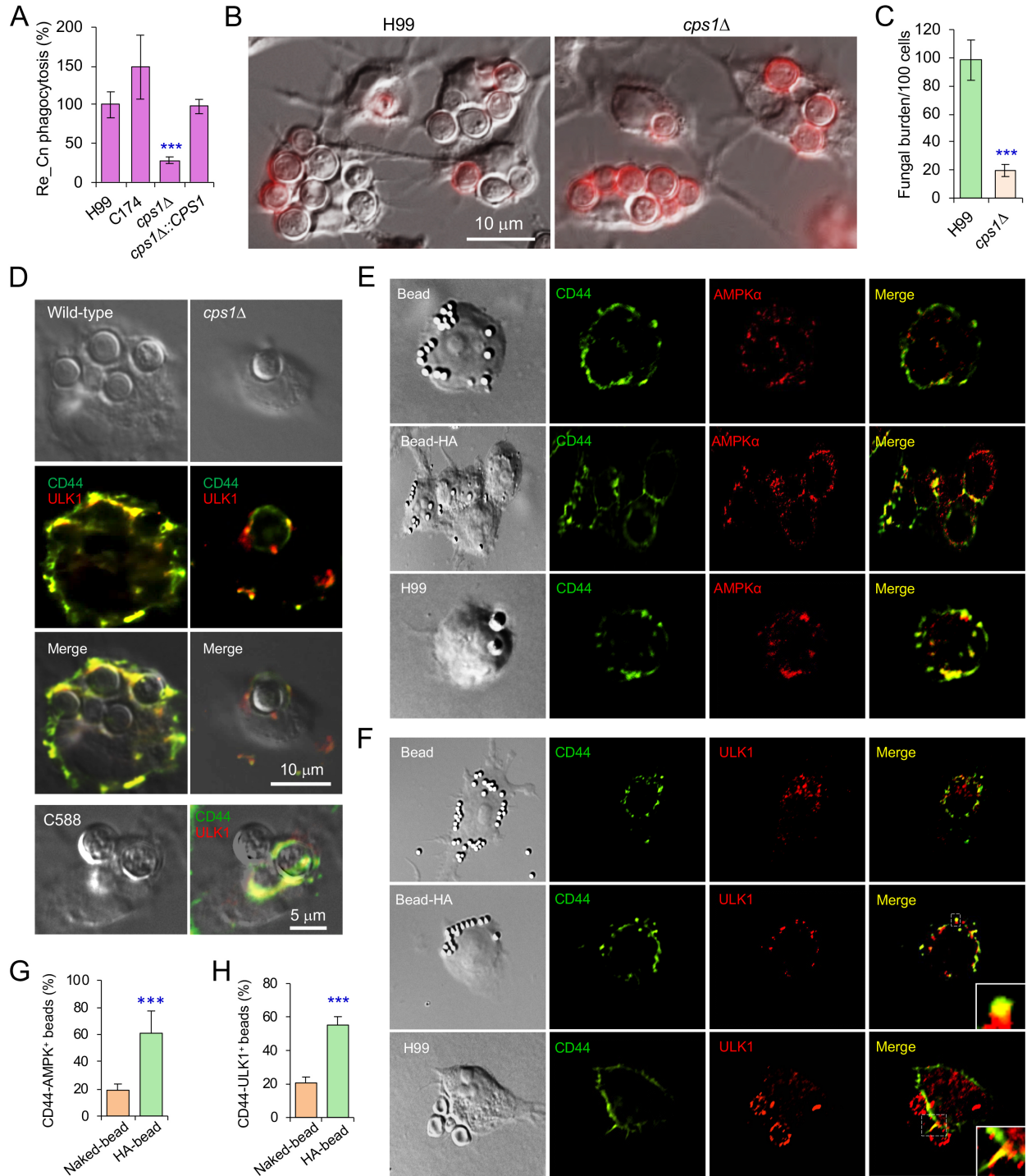
7 (B) Colocalization of CD44 with the indicated AIC components in the vicinity of nascent CnCVs
8 in host cells infected with the indicated Cn strains.

9 (C) The fluorescence intensity profile of CD44 (red) and AIC components (ATG9 or ULK1)
10 (green) along the two crossed white lines shown in the insets from (B, Merge 1).

11 (D) AMPK recruitment to nascent CnCVs in CD44 knockout (KO, CD44^{-/-}) and WT (CD44^{+/+})
12 bone marrow-derived macrophages (BMDMs) at 3 h.p.i..

13 (E, F) Cn internalization in CD44 WT and KO BMDMs infected by Cn H99 assessed using image
14 analysis approaches (E) and corresponding quantification (F) at 3 h.p.i.. Data represent the means
15 \pm standard deviation (SD) from three independent experiments. ***: significance at $p < 0.001$.

16



1
2

1 **Figure 3. Fungal HA is required for recruitment of AMPK or AIC components to nascent**
2 **phagosomes and Cn internalization.**

3 (A) Internalization of the wild-typ, *cps1Δ* and complemented Cn strains.

4 (B-C) Internalization of the indicated Cn strains in BMDMs (B) and quantification of intracellular
5 Cn cells (C) at 3 h.p.i..

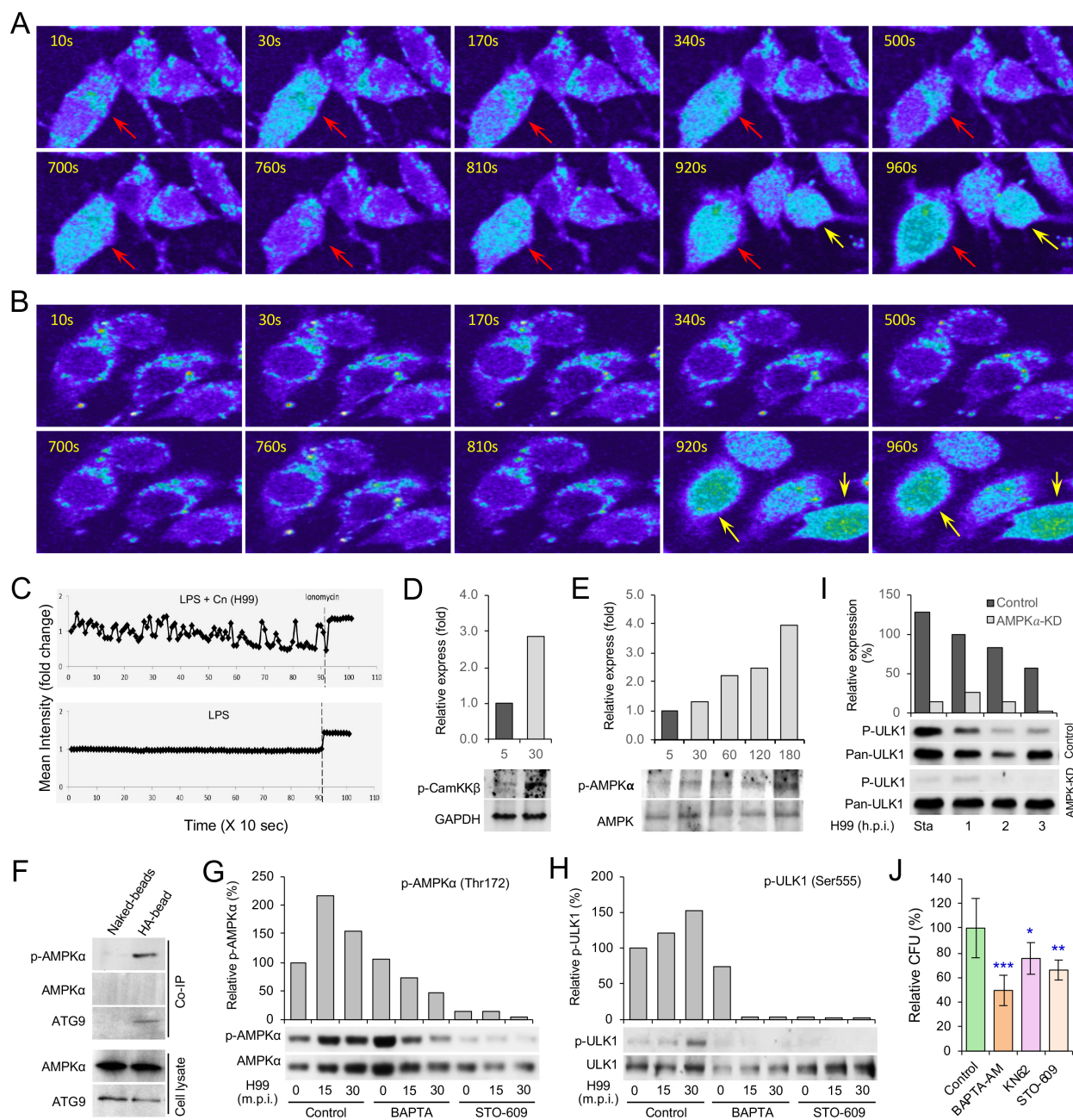
6 (D) Confocal microscopy image analysis of recruitment of CD44 and the AIC component ULK1
7 by wild-type, *cps1Δ*, and complemented (C588) Cn strains at 3 h.p.i..

8 (E-F) Recruitment of host CD44 and AMPK α (E), or CD44 and AIC component ULK1 (F) to
9 nascent phagosomes or CnCVs by HA-coated beads or Cn (H99), respectively.

10 (G, H) Quantification of CD44 and AMPK positive beads (G) or CD44 and ULK1 positive beads
11 based on confocal microscopy images as shown in (E-F). Data represent the means \pm SD from
12 three independent experiments. ***: significance at $p < 0.001$.

13

14



1
2

1 **Figure 4. Cn infection activates CaMKK β -AMPK-ULK1 signaling axis.**

2 (A, B) Cn infection results in intracellular Ca²⁺-flux in the infected host cells. Host cells incubated
3 with *cpsI*⁺ Cn (A) or PBS (B) and the intracellular Ca²⁺ level was detected by excitation at 340 nm.
4 Red arrows: Ca²⁺ releases from *cpsI*⁺-Cn-infected host cells. Yellow arrows: Ca²⁺ releases from
5 cells treated with ionomycin, a membrane permeable calcium ionophore used to increase
6 intracellular calcium levels.

7 (C) Mean Ca²⁺ flux intensity of Cn-infected (upper panel) and control (lower panel) cells.

8 (D, E) Activation of host CaMKK β (D) and AMPK α (E) in cells incubated with HA or HA-coated
9 beads.

10 (F) Co-immunoprecipitation (Co-IP) assays of host phosphorylated AMPK α and ATG9 triggered by
11 HA-coated beads. Host cells were incubated with Cn. At 3 h.p.i., the infected cells were lysed and
12 immunoprecipitated using antibodies against CD44. the precipitated material was then visualized
13 by Western blot analysis using antibodies directed against p-AMPK α or ATG9.

14 (G, H) Chelation of intracellular Ca²⁺ by BAPTA-AM and inhibition of the activity of CaMKK β
15 by STO-609 reduce activation of AMPK α (G) and ULK1 (H).

16 (I) Depletion of AMPK α reduces activation of ULK1 during Cn internalization. Sta: starvation.

17 (J) Cn internalization in host cells treated by the indicated drug via CFU assays. Data represent the
18 means \pm SD from three independent experiments. *, **, ***: significance at p < 0.05, 0.01, and
19 0.001, respectively.

20

1 Star Methods

2 KEY RESOURCES TABLE

REAGENT or RESOURCE	SOURCE	IDENTIFIER
Antibodies		
Mouse anti- <i>C. neoformans</i> 18B7	Dr. Arturo Casadevall, (Albert Einstein College of Medicine of Yeshiva University, NY, USA)	N/A
Mouse anti-HCAM(CD44)	Santa Cruz Biotechnology, Inc. (Dallas, TX USA)	Cat. #: sc-7297
anti-pCaMKK β	Cell Signaling Technology, Inc. (Danver, MA USA)	Cat #:16737S
anti-CaMKK α	Santa Cruz Biotechnology, Inc. (Dallas, TX USA)	Cat #: sc-11370/17827
anti-CaMKK β	Santa Cruz Biotechnology, Inc. (Dallas, TX USA)	Cat. #: sc-271674
Rabbit anti-pAMPK α (Thr 172)	Cell Signaling Technology, Inc. (Danver, MA USA)	Cat. #: 2535
Rabbit anti-AMPK α	Cell Signaling Technology, Inc. (Danver, MA USA)	Cat. #: 5831
Rabbit-anti pULK1 (Ser 555)	Cell Signaling Technology, Inc. (Danver, MA USA)	Cat. #: 5869
Rabbit anti-ULK1	Santa Cruz Biotechnology, Inc. (Dallas, TX USA)	Cat. #: sc-33182
Rabbit anti-LC3	Santa Cruz Biotechnology, Inc. (Dallas, TX USA)	Cat. #: sc-134226
Rabbit anti-GAPDH	Santa Cruz Biotechnology, Inc. (Dallas, TX USA)	Cat. #: sc-25778
Rabbit anti-ATG13	Sigma-Aldrich, Inc. (St. Louis, MO USA)	Cat. #: SAB4200100
Rabbit anti-FIP200	Proteintech Group, Inc. (Rosemont, IL USA)	Cat. #: 17250-1-AP
Rabbit anti-AMPK β	Novus Biologicals, Inc. (Littleton, CO USA)	Cat. #: NBP1-87487
Rabbit anti-pLKB1 (Ser428)	Abcam, Inc. (Cambridge, MA USA)	Cat. #: Ab63473
Rabbit anti-pAMPK (Thr172)-PE	BIOSS, Inc. (Woburn, MA USA).	Cat. #: BS-4002RP
Rabbit anti-pATG1 (Ser556)-PE	BIOSS, Inc. (Woburn, MA USA)	Cat. #: ABIN746733
Fungal, Bacterial and Virus Strains		
<i>C. neoformans</i> strain H99	Dr. Xiaorong Lin (Texas A&M University, College Station, TX)	N/A
<i>C. neoformans</i> strain AI100-dsRed	Dr. Xiaorong Lin (Texas A&M University, College Station, TX)	N/A
<i>C. neoformans</i> strain cap59	Dr. Xiaorong Lin (Texas A&M University, College Station, TX)	N/A
<i>C. neoformans</i> strain C177	Dr. Jong, A. (University of California, Los Angeles, CA, USA)	N/A
<i>C. neoformans</i> strain <i>cps1</i> Δ	Dr. Jong, A. (University of California, Los Angeles, CA, USA)	N/A
<i>C. neoformans</i> strain C588	Dr. Jong, A. (University of California, Los Angeles, CA, USA)	N/A
Chemicals, Peptides, and Recombinant Proteins		
STO-609	Sigma-Aldrich, Inc. (St. Louis, MO USA)	Cat. #: S1318-5MG
BAPTA-AM	Sigma-Aldrich, Inc. (St. Louis, MO USA)	Cat. #: A1076-25MG
KN62	Sigma-Aldrich, Inc. (St. Louis, MO USA)	Cat. #: I2142-1MG
RIPA buffer	G-Biosciences (San Diego, CA USA)	Cat. #: 786-489
Phosphatase inhibitor cocktail 2	Sigma-Aldrich, Inc. (St. Louis, MO USA)	Cat. #: P5726
Phosphatase inhibitor cocktail 3	Sigma-Aldrich, Inc. (St. Louis, MO USA)	Cat. #: P0044
Amino-polystyrene Particles	Spherotech, Inc. (Lake Forest, IL, USA)	Cat #: AP-10-10
Hyaluronic acid	Santa Cruz Biotechnology, Inc. (Dallas, TX USA)	Cat #: sc-337865
EDC hydrochloride	Santa Cruz Biotechnology, Inc. (Dallas, TX USA)	CAS #: 25952-53-8
pENTR4-eGFP-C1 entry vector	Addgene (Cambridge, MA, USA)	Plasmid #17396

pLenti-PGK-Neo destination vector	Addgene (Cambridge, MA, USA)	Plasmid #19067
psPAX2	Addgene (Cambridge, MA, USA)	Plasmids #12260
pMD2G/VSV-G	Addgene (Cambridge, MA, USA)	Plasmids #12259
G418	Invivogen (San Diego, CA, USA)	Cat #: NC9227938
Lipofectamine™ 2000	Invitrogen (Carlsbad, CA, USA)	Cat #: 11668027
Critical Commercial Assays		
Phagocytosis Assay Kit (IgG FITC)	Cayman Chemical, Inc. (Ann Arbor, MI USA)	Cat. #: 500290
Fe-NTA column	Thermo Fischer Scientific (Waltham, MA USA)	Cat. #: 88300
Pierce ECL Plus chemiluminescence kit	Thermo Fischer Scientific (Waltham, MA USA)	Cat. #: 32132X3
Experimental Models: Cell Lines		
RAW264.7 cells	ATCC (Manassas, VA USA)	TIB-71
J774A.1 cells	ATCC (Manassas, VA USA)	TIB-67
GFP-Gal8 (RAW264.7 macrophages)	This work	NA
GFP-LC3 (RAW macrophages)	Dr. Douglas Green (St. Jude Children's Research Hospital, Pittsburgh, PA USA)	NA
B6J2 cells	Dr. J. Suttles (University of Louisville, Louisville, KY USA)	(Sag et al., 2008)
B6J2 cells (AMPK α -DN)	Dr. J. Suttles (University of Louisville, Louisville, KY USA)	(Sag et al., 2008)
Experimental Models: Organisms/Strains		
C57BL/6 wild-type (WT) mice	Jackson Laboratories, Inc. (Bar Harbor, ME USA)	Stock No: 000664
CD44-KO mice (B6.129 (Cg)- <i>Cd44^{tm1Hbg/J}</i>)	Jackson Laboratories, Inc. (Bar Harbor, ME USA)	Stock #: 005085

1

2 CONTACT FOR REAGENT AND RESOURCE SHARING

3

4 Further information and requests for resources and reagents should be directed to and will be
5 fulfilled by the Lead Contact, Paul de Figueiredo (pjdefigueiredo@tamu.edu).

6

7 EXPERIMENTAL MODEL DETAILS

8 Bone marrow-derived macrophage harvest and cultivation

9 Bone marrow cells were collected from the femurs of littermate control and CD44 KO mice, and
10 cultivated in L929-cell conditioned media [DMEM medium containing 20% L929 cell supernatant,
11 supplemented with 10% (v/v) FCS, penicillin (100 U/ml), and streptomycin (100 U/ml)]. After 3
12 days of culture, non-adherent precursors were washed away and the retained cells were propagated
13 in fresh L929-cell conditioned media for another 4 days. For experimentation, BMDMs were split
14 in 24-well plates at a density of 2.5×10^5 cells per well in L929-cell conditioned media and
15 cultured at 37°C with 5% CO₂ overnight before use.

16

1 **Method Details**

2

3 ***Cryptococcus* Strains, Cell Culture, *Cryptococcus* Infection, and CFU Assay**

4 Yeast forms of Cn cells were cultured on YPD (Difco™) agar plates and maintained on the plates
5 for 4 to 5 days prior to experimentation. Mammalian cell lines were routinely incubated in DMEM
6 supplemented with 10% FBS in a 5% CO₂ atmosphere at 37°C. Preparation of cryptococcal and
7 host cells for infection as well as CFU assays that measured internalized Cn cells were performed
8 as previously described (Qin et al., 2011; Pandey et al., 2017).

9

10 **Immunofluorescence Microscopy Assays for Cn Phagocytosis**

11 Mammalian host cells were first cultivated on 12 mm glass coverslips (Fisherbrand) on the bottom
12 of 24-well plates (Falcon) for 12-16 h before infection. Next, the host cells were infected with the
13 tested Cn cells and incubated at 37°C in a 5% CO₂ atmosphere. At the indicated time points post-
14 infection, culture media was removed and the infected host cells were washed 6 to 8 times with
15 PBS (pH 7.4) before being fixed with 3.7% formaldehyde. The fixed cells were then processed Cn
16 phagocytosis assays using antibody (18B7) directed against Cn as previous described (Qin et al.,
17 2011; Pandey et al., 2017) without adding Triton X-100 to the staining buffer. The numbers of
18 internalized (unstained) and extracellular (stained) Cn cells were then quantified and plotted.
19 Images represent a representative image from triplicate replicates, with 100 fields imaged per
20 replicate.

21

22 **Drug/compound Treatments**

23 Murine macrophage J774.A1 or RAW264.7 cells were overnight cultured in 48 well plates and
24 then coincubated with assorted pharmacological compounds, including KN62, STO-609 or
25 BAPTA-AM for 3 h. The media containing the compounds was then removed. For CFU assays,
26 the drug-treated cells were extensively washed with fresh medium and then infected with Cn cells.
27 At 3 h.p.i., the infected cells were lysed and performed CFU assay as previously described (Qin
28 et al., 2011; Pandey et al., 2017). For western blots, the compound-treated cells were washed 3
29 times with cold 1 × PBS, pH7.4, lysed and performed immunoblotting assay as previously
30 describe (Pandey et al., 2017).

31

1 **Lentivirus-Mediated Depletion of Host Proteins**

2 The pSuperRetro retroviral vector system (OligoEngine, Inc.) was used to knockdown target gene
3 expression in murine cells according to the manufacturer's instructions. The oligonucleotides used
4 for shRNA construction to knockdown the expression of mouse genes and the accompanying
5 references are listed in **Table S1**. Transfection was performed in 6-well plates containing
6 1.5×10^5 RAW264.7 or B6J2 cells. Clones with the insert stably integrated were selected with
7 puromycin. Western blot was performed to validate the depletion of the targeted proteins. All
8 Westerns were performed in triplicate and representative findings are shown.

10 **Generation of GFP-tagged Gal8 RAW264.7 cells**

11 The GFP-galectin-8 expression construct was made by first cloning the cDNA sequence of *Lgals8*
12 (from RAW 264.7 cells) into the pENTR4-eGFP-C1 entry vector (Campeau et al., 2009), resulting
13 in a fusion of eGFP on the N-terminus of galectin-8. This construct was fully Sanger sequenced
14 (Eton Biosciences, San Diego, CA) to verify the fusion protein was in-frame and error-free. GFP-
15 Gal8 was then Gateway cloned with LR Clonase (Invitrogen) into the pLenti-PGK-Neo
16 destination vector (Campeau et al., 2009). Lenti-X 293T cells (Takara Bio) were co-transfected
17 with pLenti-GFP-Gal8 and the packaging plasmids psPAX2 and pMD2G/VSV-G (Addgene
18 Plasmids #12259-60) to produce lentiviral particles. RAW 264.7 cells were transduced with GFP-
19 Gal8 lentivirus for two consecutive days plus 1:1000 Lipofectamine 2000 (Invitrogen) and
20 selected for 5 days with 750 $\mu\text{g/ml}$ G418 (Invivogen). Expression of GFP-Gal8 was confirmed by
21 Western blot analysis and fluorescence microscopy.

23 **Confocal Microscopy Assays**

24 Host cells were infected with live or heat killed, opsonized or unopsonized capsular or acapsular
25 strains of Cn. At the indicated times post-infection, host cells were fixed for confocal
26 immunofluorescence microscopy analysis using antibodies directed against the indicated host
27 proteins. Immunofluorescence microscopy staining and imaging methods (Qin et al., 2008; Qin
28 et al., 2011; Pandey 2017; Pandey 2018) were used to determine the subcellular localization of
29 host AIC components in infected host cells. Samples were observed on a laser scanning confocal
30 microscope or on a confocal fluorescence microscope (ECLIPSE Ti, Nikon). Confocal images
31 ($1,024 \times 1,024$ pixels) were acquired and processed with NIS elements AR 3.0 software (Nikon)

1 and assembled with Adobe Photoshop CC 2019 (Adobe Systems, CA, USA). Digital image
2 analysis and quantification was performed as previously described (Qin et al., 2011). Findings
3 from our subcellular localization analyses were not an artifact of secondary antibody cross
4 reactivity with host or pathogen components because negligible fluorescence signal was observed
5 when infected cells were stained with secondary antibodies alone, or the pathogen alone was
6 stained with the antibodies used in the experiments (**Figure S4G**).

7 8 **Protein pull-down assay with HA-coated or naked beads**

9 Spherical amino polystyrene beads (size: 1.0-1.4 μm , Spherotech Inc, IL, USA) were covalently
10 coupled using EDC [*N*-Ethyl-*N'*-(3-dimethylaminopropyl)carbodiimide hydrochloride] to
11 hyaluronic acid (HA) (Santa Cruz Biotech.) as per the manufacturer's (Spherotech) instruction.
12 Briefly, 200 μl of 0.05 M sodium acetate buffer (pH 5.0), 2 mg of HA, 2 ml of 5% w/v Amino
13 particles and 20 mg of EDC were mixed in a glass centrifuge tube. The contents were vortexed
14 and incubated for 2 hrs at ambient temperature on a rotary mixer. Following incubation, the tube
15 was centrifuged at 3000 \times g for 15 minutes and supernatant was carefully discarded. The pellet
16 was washed twice in 1 \times PBS and resuspended in 2 ml of 1 \times PBS to obtain 5% w/v suspension of
17 HA coated beads. RAW 264.7 cells (3×10^5) were washed with 1 \times PBS. Next, a bead incubation
18 solution containing 5 μl of HA-coated or naked beads in 200 μl of PBS was added to the washed
19 cells. The cells were centrifuged for 10 min at 1500 RPM and then incubated in a humidified
20 incubator containing 5% CO₂ for 2 hrs. The treated cells were washed 2-4 times with ice-cold 1
21 \times PBS and lysed in 80 μl RIPA buffer supplemented with a cocktail of protease and phosphatase
22 inhibitors. Beads were separated from the lysate by high-speed centrifugation at 4°C. The
23 separated beads were washed 3 times with RIPA buffer and finally resuspended in 80 μl RIPA
24 buffer and 20 μl of 5 \times sample buffer (Thermo Scientific) and boiled for 5 mins. Samples were
25 finally resolved by SDS-PAGE and subjected to western blot analysis.

26 27 **Immunoblotting Analysis**

28 Preparation of protein samples and western blot analysis were performed as described previously
29 (Qin et al., 2011; Pandey et al., 2017; Pandey et al., 2018). Blot densitometry was performed using
30 the ImageJ (<http://rsbweb.nih.gov/ij/>) software package. All Westerns were performed in triplicate
31 and representative findings are shown.

1
2 **Quantification and Statistical Analysis**
3 The quantitative data presented in this work represent the mean \pm standard deviation (SD) from at
4 least three independent experiments. To easily compare results from independent experiments, the
5 data from controls, such as protein expression level, blot densitometry, CFU, intracellular Cn
6 number, etc., were normalized as 1 or 100%. The significance of the data was assessed using the
7 Student's *t*-test to assess statistical significance between two experimental groups or a one-way
8 ANOVA test to evaluate the statistical differences of multiple comparisons of the data sets.
9

Supplemental Figures and Figure Legends

Interactions between fungal hyaluronic acid and host CD44 promote internalization by recruiting host autophagy proteins to forming phagosomes

Sheng Li Ding^{1,2,6}, Aseem Pandey^{2,3,6}, Xuehuan Feng^{2,6}, Jing Yang², Luciana Fachini da Costa^{2,4}, Roula Mounceimne³, Allison Rice-Ficht⁴, Samantha L. Bell⁵, Robert O. Watson⁵, Kristin Patrick⁵, Qing-Ming Qin^{1,2*}, Thomas A. Ficht^{3*}, Paul de Figueiredo^{2,3,7*}

¹ College of Plant Sciences & Key Laboratory of Zoonosis Research, Ministry of Education, Jilin University, Changchun 130062, Jilin, China; Department of Plant Pathology, College of Plant Protection, Henan Agricultural University, Zhengzhou 450002, Henan, China

² Department of Microbial Pathogenesis and Immunology, Texas A&M Health Science Center, Norman Borlaug Center, Texas A&M University, College Station, Texas 77843, USA

³ Department of Veterinary Pathobiology, Texas A&M University, College Station, Texas 77843, USA

⁴ Department of Molecular and Cellular Medicine, College of Medicine, Texas A&M Health Science Center, College Station, Texas 77843, USA

⁵ Department of Microbial Pathogenesis and Immunology, Texas A&M Health Science Center, Bryan, Texas 77807, USA

⁶ These authors contributed equally

⁷ Lead contact

* Correspondence: qm Qin@jlu.edu.cn (Q.M.Q.), tficht@tamu.edu (T.A.F.), pjdefigueiredo@tamu.edu (P.d.F.)

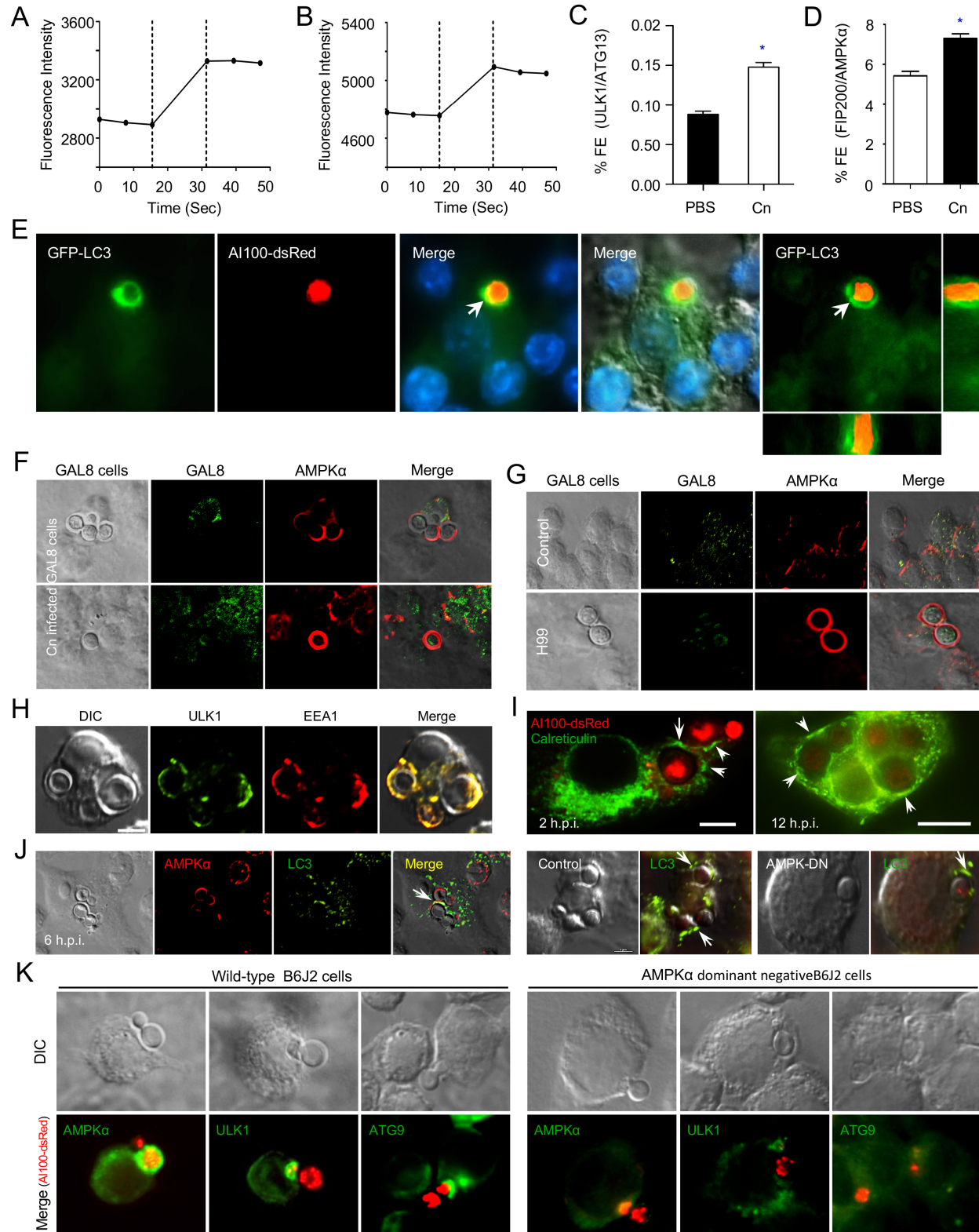


Figure S1. Recruitment of AIC components, but not galectin 8, to nascent phagosomes during Cn internalization.

(A, B) Fluorescence intensity of ULK1 and ATG13 (A) or FIP200 and AMPK α (B) during Cn internalization.

(C, D) Interactions between host ULK1 and ATG13 (C) or FIP200 and AMPK α (D) recruited to Cn-containing vacuoles (CnCVs) in RAW264.7 macrophages. The infected host cells were quantified using FRET analysis. Data represent the means \pm standard deviations (SD) from at least three independent experiments. * indicates significance at $P < 0.05$.

(E) Recruitment of host LC3 to the nascent CnCVs during Cn internalization.

(F, G) Host galectin 8 is not recruited to nascent phagosomes containing Cn cells during Cn internalization by host cells expressing GFP-galectin 8 (F) or cells supplemented with UBEI-41, a cell permeable inhibitor of ubiquitin-activating enzyme E1 (G).

(H) Colocalization of host early endosomal marker EEA1 with AIC component ULK1 surrounding nascent CnCVs.

(I) Recruitment of host endoplasmic reticulum marker calreticulin to nascent and formed CnCVs.

(J) Recruitment of host AMPK α and LC3 to nascent phagosomes containing Cn cells in infected bone marrow derived macrophages (BMDMs, left panel) or in B6J2 macrophages expressing dominant negative variant of AMPK α (AMPK-DN) and control (right panel).

(K) Less recruitments of host AMPK α and AIC component ULK1 or ATG9 to nascent CnCVs in B6J2 macrophages expressing dominant negative AMPK α variant during Cn internalization.

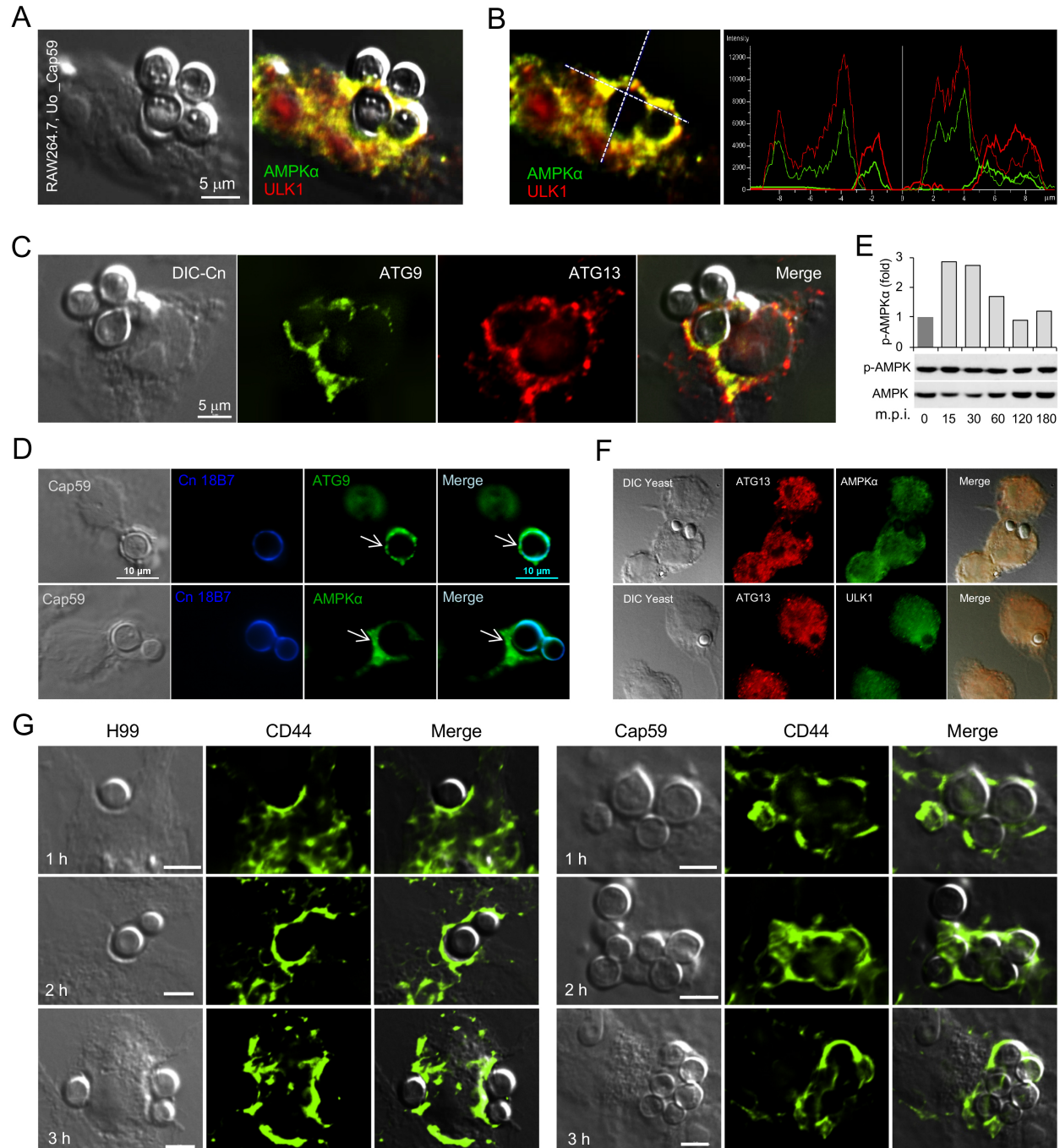


Figure S2. Recruitment of host AIC components and CD44 to forming or nascent CnCVs during Cn internalization.

- (A) Recruitment of AMPK α and AIC components ULK1 to nascent CnCVs.
- (B) The fluorescence intensity profile of AMPK α (green) and ULK1 (red) along the two crossed white lines (left panel).
- (C) Colocalization of ATG9 with ATG13 in the vicinities of CnCVs.
- (D) Colocalization of host AMPK α or ATG9 with cryptococcal glucuronoxylomannan (GXM)-specific monoclonal antibody 18B7.
- (E) Activation of host AMPK α by heat-killed (HK) Cn cells (cap 59) during phagocytosis. Representative results from one of three independent experiments are shown.
- (F) Recruitment of AIC components and AMPK α to nascent phagosomes is hardly detected during phagocytosis of yeast (*Saccharomyces cerevisiae*) cells by host cells.
- (G) Recruitment of CD44 during a time course (3 hr) of Cn internalization.

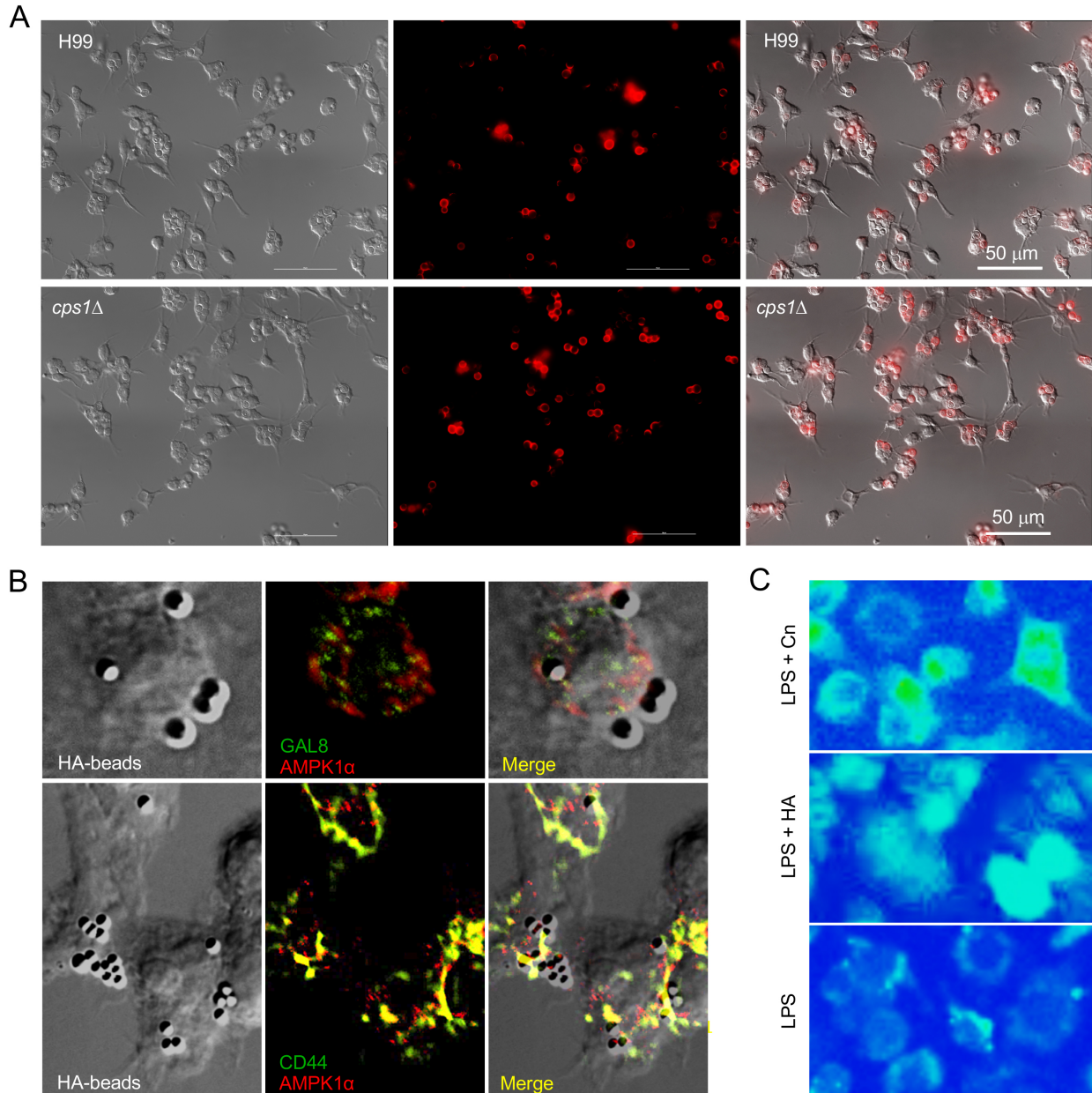


Figure S3. Fungal hyaluronic acid (HA) is required for Cn internalization.

(A) Disruption of Cn *cps1* impairs internalization of the fungal pathogen (related to Figure 3B-C).

(B) Recruitment of CD44, not galectin 8, to the forming or nascent phagosomes associated with HA-coated beads. Upper panel: localization of galectin 8 and AMPKα in cells incubated with HA-coated beads. Low panel: colocalization of CD44 and AMPKα to the forming or nascent phagosomes related to HA-coated beads.

(C) Incubation of host cell with Cn harboring *cps1* (top) or HA (middle) increases intracellular Ca²⁺ level (excited at 340 nm).

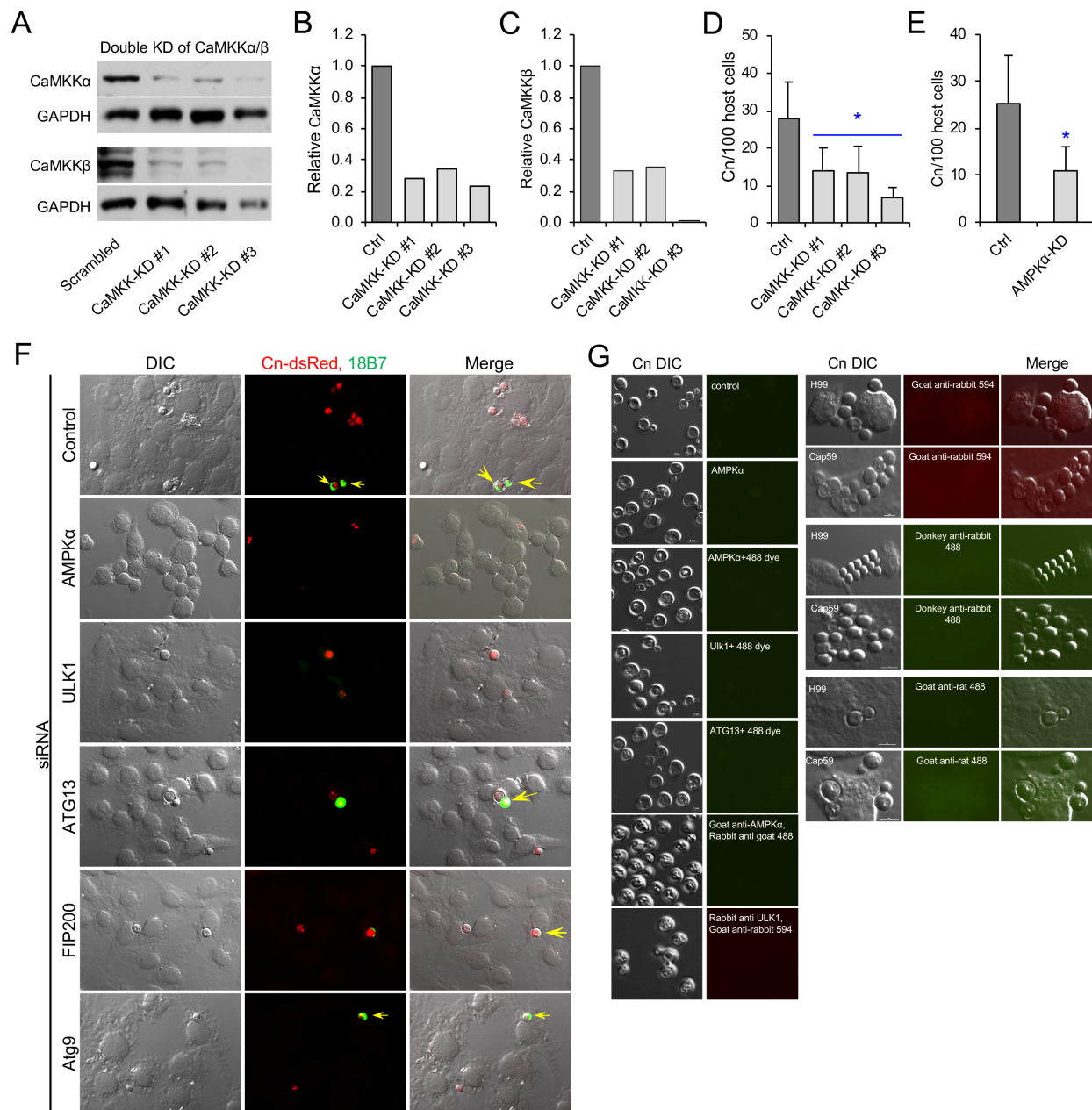


Figure S4. Components in the CaMKK -AMPK-ULK1 signal axis play important roles in Cn internalization.

(A) Immunoblotting assay to test the depletion of CaMKK α/β protein level by the shRNA approach.

(B, C) Relative protein expression levels of CaMKK α (B) or CaMKK β (C) in RAW macrophages transfected with scrambled or CaMKK α/β shRNAs. Data from a representative experiment shown in (A).

(D, E) Depletion of host cell CaMKK α/β (D) or AMPK α (E) reduces Cn internalization determined by immunofluorescence microscopy assay. Data represent the means \pm SD from three independent experiments. *: significance at $p < 0.05$.

(F) Depletion of host cell AMPK α and AIC components reduces Cn internalization determined by immunofluorescence microscopy assay. Images from a representative experiment of three independent experiments.

(G) Cn cells harvested from infected host cells (left panel) or during host infection (right panel) do not display cross activities with the primary or secondary antibodies used in this work.

Table S1. shRNAs and PCR primers used in this study

shRNA ID	Sequence (5'-3')	References
shCaMKK α 1	GGAAGTGCCCGTTCATTGATT	This study
shCaMKK α 2	TCAATGGCTGAGGTGAGGCAC	This study
shCaMKK β 1	GGTGCTGTCCAAAAGAAA	This study
shCaMKK β 2	TTGCGTAATAAGTATTGTCAT	This study
shFIP200	GAGAGAACTTGTTGAGAAA	Pandey et al., 2017
	ACATGAAGGCTCAGAGAAA	ditto
shUlk1	GAGCAAGAGCACACGGAA A	ditto
	AGACTCCTGTGACACAGAT	ditto
shAtg13	GAGAAGAATGTCCGAGAAT	ditto
	ACAGGAAGGACTTGGACAA	ditto
shPrkaa1	TGAATTAACCCACAGAAA	ditto
	GGTCATCAGTACACCATCT	ditto
shPrkab1	TGAACAAGGACACGGGCAT	ditto
	GCACGACCTGGAAGCGAAT	ditto
Scramble 1	ATTGTATGCGATCGCAGAC	ditto
Scramble 2	CACCAGCATCTGATCTAGA	ditto
Ulk1-F1	ACTGCGGCCGCatggattacaaggatgacgatgacaagatggag ccgggccgcgcggc	ditto
Ulk1-r1	GAAGAATTCtcaggcatagacaccactcag	ditto
ULK1-F2	GATCTGGATCCGGAGTCGACGGAGCGGCCGCatggatta caagga	ditto
Ulk1-R2	AGCGCCTCCCCTACCCGGTAGAATTCtcaggcatagaca ccactc	ditto
Atg13-F1	ACTAGATCTATGTACCCATACGATGTTCCAGATTACGCT ATGGAACTGAACTCAGCTCC	ditto
Atg13-R1	GAACTCGAGTTACTGCAGGGTTTCCACAAA	ditto
Atg13-F2	ACTCCTTCTCTAGGCGCCGGAATTAGATCTATGTACCCA TACGAT	ditto
Atg13-R2	ACCCGGTAGAATTCGTTAACCTCGAGttactgcagggtt tccaca	ditto
Prkaa1-F1	ACTGCGGCCGCATGGTGAGCAAGGGCGAGGAGCTGTTCA	ditto
Prkaa1-R1	GAAGAATTCCTTACTGTGCAAGAATTTTAAT	ditto
Prkaa1-F2	GATCTGGATCCGGAGTCGACGGAGCGGCCGCATGGTGAG CAAGGG	ditto
Prkaa1-R2	AGCGCCTCCCCTACCCGGTAGAATTCttactgtgcaaga atttta	ditto